




## Article

# Caffeic Acid in Spent Coffee Grounds as a Dual Inhibitor for MMP-9 and DPP-4 Enzymes

Enade P. Istyastono <sup>1,\*</sup>, Nunung Yuniarti <sup>2</sup>, Vivitri D. Prasasty <sup>3</sup>, Sudi Mungkasi <sup>4</sup>, Stephanus S. W. Waskitha <sup>1</sup>, Michael R. S. Yanuar <sup>1</sup> and Florentinus D. O. Riswanto <sup>1</sup>

- <sup>1</sup> Research Group of Computer-Aided Drug Design and Discovery of Bioactive Natural Products, Faculty of Pharmacy, Sanata Dharma University, Yogyakarta 55282, Indonesia; s.waskitha@usd.ac.id (S.S.W.W.); gregoriusrest@gmail.com (M.R.S.Y.); dikaocta@usd.ac.id (F.D.O.R.)
- <sup>2</sup> Department of Pharmacology and Clinical Pharmacy, Faculty of Pharmacy, Universitas Gadjah Mada, Yogyakarta 55281, Indonesia; nunung@mail.ugm.ac.id
- <sup>3</sup> Department of Pathobiological Sciences, School of Veterinary Medicine, Louisiana State University, Baton Rouge, LA 70803, USA; vprasasty@lsu.edu
- <sup>4</sup> Department of Mathematics, Faculty of Science and Technology, Sanata Dharma University, Yogyakarta 55282, Indonesia; sudi@usd.ac.id
- \* Correspondence: enade@usd.ac.id; Tel.: +62-274-883037

**Abstract:** Type 2 diabetes mellitus and diabetic foot ulcers remain serious worldwide health problems. Caffeic acid is one of the natural products that has been experimentally proven to have diverse pharmacological properties. This study aimed to assess the inhibitory activity of caffeic acid and ethanolic extract of spent coffee grounds targeting DPP-4 and MMP-9 enzymes and evaluate the molecular interactions through 50-ns molecular dynamics simulations. This study also introduced our new version of PyPLIF HIPPOS, PyPLIF HIPPOS 0.2.0, which allowed us to identify protein–ligand interaction fingerprints and interaction hotspots resulting from molecular dynamics simulations. Our findings revealed that caffeic acid inhibited the DPP-4 and MMP-9 activity with an IC<sub>50</sub> of 158.19 ± 11.30 μM and 88.99 ± 3.35 μM while ethanolic extract of spent coffee grounds exhibited an IC<sub>50</sub> of 227.87 ± 23.80 μg/100 μL and 81.24 ± 6.46 μg/100 μL, respectively. Molecular dynamics simulations showed that caffeic acid interacted in the plausible allosteric sites of DPP-4 and in the active site of MMP-9. PyPLIF HIPPOS 0.2.0 identified amino acid residues interacting more than 10% throughout the simulation, which were Lys463 and Trp62 in the plausible allosteric site of DPP-4 and His226 in the active site of MMP-9.

**Keywords:** type 2 diabetes mellitus; diabetic foot ulcers; caffeic acid; molecular dynamics simulations; PyPLIF HIPPOS 0.2.0



**Citation:** Istyastono, E.P.; Yuniarti, N.; Prasasty, V.D.; Mungkasi, S.; Waskitha, S.S.W.; Yanuar, M.R.S.; Riswanto, F.D.O. Caffeic Acid in Spent Coffee Grounds as a Dual Inhibitor for MMP-9 and DPP-4 Enzymes. *Molecules* **2023**, *28*, 7182. <https://doi.org/10.3390/molecules28207182>

Academic Editor: Domenico Trombetta

Received: 5 September 2023

Revised: 5 October 2023

Accepted: 17 October 2023

Published: 19 October 2023



**Copyright:** © 2023 by the authors. Licensee MDPI, Basel, Switzerland. This article is an open access article distributed under the terms and conditions of the Creative Commons Attribution (CC BY) license (<https://creativecommons.org/licenses/by/4.0/>).

## 1. Introduction

Type 2 diabetes mellitus (T2DM) is a metabolic disorder characterized by chronically increased blood glucose, insulin, and the dysfunction of pancreatic β-cells [1,2]. T2DM is also commonly associated with diabetic foot ulcers (DFU), which is a complication of severe and not well-controlled T2DM [3]. The International Diabetes Federation reported that about 537 million adults were living with diabetes in 2021, of whom more than 90% of people suffered from T2DM; this disease is estimated to rise in 2030 and 2045 [4]. Many treatments have been developed to cope with T2DM and DFU, including the utilization of natural products and their extracts [5–7]. As time goes by, natural products have played a pivotal role due to their ability to interact with various targets, leading to a significant contribution to drug discovery [8].

Caffeic acid, (*E*)-3-(3,4-dihydroxyphenyl)prop-2-enoic acid, is a phenolic compound that has widely been found in several agricultural products such as vegetables, fruits, carrots, tea, coffee beans, and spent coffee grounds [9,10]. Several experiments have

documented that caffeic acid exhibited an extensive range of biological activities such as antioxidant [11], antiviral [12], anticancer [13], antiplasmodial [14], and antidiabetic properties [15,16]. Previous studies have found that caffeic acid has various diabetes-relieving mechanisms, including improving glucose homeostasis as well as pancreatic  $\beta$ -cell function [16], suppressing hepatic nuclear factor-4 (HNF-4), and decreasing phosphoenolpyruvate carboxykinase (PEPCK) activity to maintain glucose homeostasis [17]. Several natural products and their extracts targeting potential receptors for diabetes treatment such as dipeptidyl peptidase-IV (DPP-4) [18] and matrix metalloproteinase-9 (MMP-9) for wound healing of DFU have been well studied and reviewed [19–22]. Our previous *in silico* study also revealed the molecular mechanism of caffeic acid in inhibiting DPP-4 and that PyPLIF HIPPOS could identify the interaction hotspots [23,24]. Yet, the molecular mechanism and interaction hotspot identification of caffeic acid as a dual inhibitor targeting DPP-4 and MMP-9 for T2DM and DFU treatment are still rarely discussed.

This study aimed to experimentally evaluate the inhibitory activity of caffeic acid and ethanolic extract of spent coffee grounds targeting DPP-4 and MMP-9 enzymes. Furthermore, a molecular mechanism of caffeic acid as a dual inhibitor of DPP-4 and MMP-9 was investigated using 50-ns molecular dynamics simulations; its interaction hotspots were identified throughout the simulation. This research also introduced our new version of PyPLIF HIPPOS, PyPLIF HIPPOS 0.2.0., which is the upgraded version of PyPLIF HIPPOS, facilitated with a feature to identify interaction fingerprints directly from the protein–ligand complex in mol2, pdb, or pdbqt formats called ‘direct IFP’. This feature was applied to the complexes resulting from molecular dynamics simulations in this research.

## 2. Results and Discussion

### 2.1. DPP-4 and MMP-9 Inhibitory Assay

Spent coffee grounds are the solid waste by-products related to coffee consumption [25]. As waste products, spent coffee grounds are reported to have several organic compound contents such as polyphenols, amino acids, minerals, polysaccharides, and fatty acids [26]. Spent coffee grounds were also reported to have several benefits to human health due to their bioactive compound content [27]. In this study, we focused on the evaluation of the activity of spent coffee grounds towards both DPP-4 and MMP-9 inhibition. Caffeic acid standard activity was also evaluated in order to present the empirical results of bioactive compound activities. Furthermore, the molecular dynamics simulations were employed to strengthen the results of the *in vitro* evaluation.

The DPP-4 inhibitory assay was performed using the DPP-4 inhibitor screening assay kit (Cayman Chemical, Ann Arbor, MI, USA). It was found that the half-maximal inhibitory concentration ( $IC_{50}$ ) of standard caffeic acid and ethanolic extract of spent coffee grounds toward DPP-4 were  $158.19 \pm 11.30 \mu\text{M}$  and  $227.87 \pm 23.80 \mu\text{g}/100 \mu\text{L}$ , respectively. The MMP-9 inhibitory assay was performed using the MMP-9 Inhibitor Screening Kit (Biovision K844-100). It was found that the  $IC_{50}$  of standard caffeic acid and the ethanolic extract of spent coffee grounds toward MMP-9 were  $88.99 \pm 3.35 \mu\text{M}$  and  $81.24 \pm 6.46 \mu\text{g}/100 \mu\text{L}$ , respectively. The lower  $IC_{50}$  value of both standard caffeic acid and ethanolic extract of spent coffee grounds towards MMP-9 compared to DPP-4 indicated the higher inhibitory activity of caffeic acid.

Compared to other known DPP-4 inhibitors such as alogliptin, sitagliptin, and omarigliptin, caffeic acid tended to have a lower inhibitory activity [28,29]. Nevertheless, it was found that caffeic acid inhibited DPP-4 with a lower  $IC_{50}$  in  $\mu\text{M}$  compared to other natural products such as hopeaphenol [30], rutin, naringin, hesperidin, and eriocitrin [18,31]. Our results also exhibited that the ethanolic extract of spent coffee grounds had a lower  $IC_{50}$  in  $\mu\text{g}/\mu\text{L}$  compared to another natural product extract such as amla fruit extract from *Emblica officinalis* fruit [32]. Several MMP-9 inhibitors have been reviewed and exhibited a higher inhibitory activity compared to caffeic acid, such as marimastat together with its analogs, and sulfonamide hydroxamic acid-based inhibitors [33]. Interestingly, caffeic acid exhibited a lower  $IC_{50}$  value in  $\mu\text{M}$  compared to other natural products such as

luteolin-7-*O*-rutinoside [34], kaempferol, morin, and taxifolin [35]. It was also discovered that the ethanolic extract of spent coffee grounds had a lower IC<sub>50</sub> value in µg/mL than another natural product extract from the previous research, namely *Hibiscus rosa-sinensis* leaves [36]. Our results proved that caffeic acid and the ethanolic extract of spent coffee grounds could potentially be dual inhibitors of DPP-4 and MMP-9 as other natural product-based inhibitors for alternative T2DM and DFU treatment. To provide a comprehensive evaluation of the inhibitory effect, the molecular dynamics study was then applied to assess the interaction stability of caffeic acid towards DPP-4 and MMP-9.

## 2.2. Molecular Docking Simulations of Caffeic Acid Targeting DPP-4 and MMP-9

Redocking of DPP-4 and MMP-9 native ligands was initially performed prior to the molecular docking simulations of caffeic acid to validate the reliability of the used molecular docking configuration. Our results exhibited that 100 redocking simulations of the native ligand of each receptor had an RMSD value of  $\leq 2.000$  Å, suggesting that the redocking configuration was reliable and could be used for molecular docking of the proposed compound, i.e., caffeic acid in the active site of DPP-4 and MMP-9.

The molecular docking simulations of caffeic acid in the active site of DPP-4 showed that all the best-docked caffeic acid had an RMSD value of  $\leq 2.000$  Å with a maximum value of 0.1183 Å, meaning that there was only one dominant pose of best-docked caffeic acid from 100 molecular docking replications. Compared to the molecular docking of caffeic acid in the DPP-4 active site, this investigation found that the best-docked caffeic acid poses in the MMP-9 active site resulted in RMSD value of  $\leq 2.000$  Å and  $> 2.000$  Å which asserted that there were more than one reasonable docking poses. In addition, it was discovered that the best-docked caffeic acid was stable enough to interact in the active site of DPP-4 with a binding affinity value of 6.707 to 6.798 kcal/mol while caffeic acid in the active site of MMP-9 also interacted nicely with a binding affinity value of 7.319 to 7.386 kcal/mol. To evaluate the interaction stability of each receptor–ligand complex, molecular dynamics simulations were performed as a further molecular docking validation since it was mentioned in the previous research [37]. In this research, the best-docked caffeic acid with the highest binding affinity was subjected to molecular dynamics simulations since it possessed the highest interaction stability.

## 2.3. Molecular Dynamics and Interaction Hotspot Identifications of Caffeic Acid-DPP-4

The interaction stability of caffeic acid in the active site of DPP-4 and the conformational stability of DPP-4 backbone atoms were evaluated based on the RMSD ligand movement (RMSD\_LigMove) and RMSD backbone, respectively, which are presented in Figure 1. According to the previous research [38], a ligand is considered to be stable if the RMSD value is below 2.000 Å. It can be clearly seen in Figure 1 that the RMSD LigMove values of caffeic acid never reached an RMSD value below 2.000 Å which indicated that caffeic acid interacted unstably in the DPP-4 active site, leading the caffeic acid explored in the DPP-4 allosteric sites to reach its maximum interaction stability [23]. The instability of caffeic acid interacting in the DPP-4 active site was presumably due to the negatively charged amino acid residues of Glu205 and Glu206 which electrostatically repelled the deprotonated caffeic acid. As reported by our previous research and Musoev et al., the active site of DPP-4 consisted of Tyr666, Tyr662, Tyr631, Tyr547, Phe357, Glu205, Glu206, and Arg125 [23,39]. Our visual inspection showed that caffeic acid still interacted with Tyr666, Tyr662, Tyr547, Phe357, Glu205, and Glu206 at the simulation time of 1.0 ns even though the RMSD LigMove value was 3.755 Å. The RMSD LigMove value increased until the simulation time reached 1.5 ns. At this time, caffeic acid interacted only with amino acid residues in the active site of Tyr547 and Phe357 with others of Pro550, Cys551, Ser552, Gln553, Trp629, and Ser630.

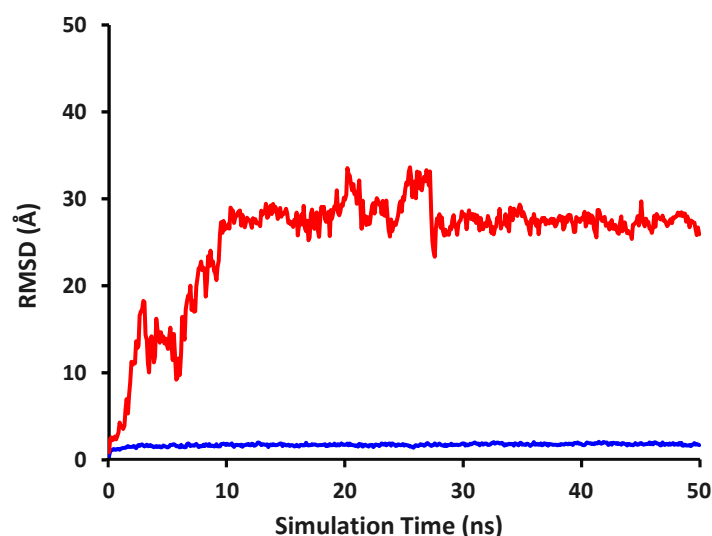


**Figure 1.** RMSD alterations of DPP-4 backbone atoms complexed with caffeic acid (blue) and RMSD ligand movement of caffeic acid (red) during 50-ns simulations.

From this simulation time, it could be seen that the RMSD LigMove value increased gradually along the simulation time until it reached 3.0 ns with an RMSD value of 18.158 Å while caffeic acid was no longer interacting with amino acid residues in the active site, revealing the availability of allosteric sites [40]. Even though there was a decreasing RMSD value reaching 9.209 Å at a simulation time of 5.7 ns, caffeic acid remained interacted in a plausible allosteric site. These results suggested that caffeic acid started escaping the active site at the simulation time of 1.5 ns to occupy more stable interactions in the plausible sites. Hence, caffeic acid might never interact stably in the DPP-4 active site and might be a non-competitive inhibitor of DPP-4 as several non-competitive inhibitors, as previously reported [40–42].

Our findings showed that caffeic acid interacted with Trp62, Ser460, and Lys463 in the plausible allosteric site at the end of the simulation. It was found that caffeic acid formed ionic, hydrogen bond, and hydrophobic interactions with Lys463. The interactions were also strengthened by amino acid residues of Trp62 along with Ser460 via hydrogen bond with the carboxylic group of caffeic acid as the acceptor and amino acid residue of Trp62 via aromatic (edge-to-face together with face-to-face). These results revealed that the carboxylic group of caffeic acid played a significant role in receptor–ligand stabilization, forming an ionic interaction with Lys463 as well as hydrogen bonds with Trp62, Ser460, and Lys463. In addition, the aromatic ring of caffeic acid formed aromatic and hydrophobic interactions with Trp62 together with Lys463, respectively.

Figure 1 also shows the altering RMSD value of DPP-4 backbone atoms having an average RMSD value of 1.714 Å. Although there were seven snapshots having an RMSD value of more than 2.000 Å, the maximum value of the RMSD backbone was only 2.062 Å, hence it may be presumed that DPP-4 backbone atoms conformations were relatively stable during 50-ns simulations. Tables 1 and 2 tabulate the amino acid residues interacting with caffeic acid for every snapshot which resulted from PyPLIF HIPPOS 0.2.0. Tables 1 and 2 show that throughout the simulation, caffeic acid interacted with amino acid residues of Lys463 (47.50%) and Trp62 (12.57%) dominantly. Our investigations found that Lys463 forming an hydrophobic interaction and Trp62 forming an aromatic edge-to-face interaction were considered as the interaction hotspots located in the DPP-4 allosteric site which predominantly strengthened the caffeic acid interaction in the DPP-4 allosteric site.

**Table 1.** Hydrophobic interaction hotspots resulted from 50-ns molecular dynamics simulations of DPP-4 interacting with caffeic acid.

Interacting Residue	Interaction Percentage
Arg61	0.80%
Trp62	1.80%
Pro159	2.40%
Pro218	1.60%
Lys463	47.50%
Tyr547	2.79%
Asn562	0.80%
Tyr631	0.60%
Tyr662	0.20%
Tyr666	1.40%

**Table 2.** Non-hydrophobic interaction hotspots resulted from 50-ns molecular dynamics simulations of DPP-4 interacting with caffeic acid.

Interacting Residue	Interaction Type	Interaction Percentage
Tyr48	Aromatic (Edge to face)	0.20%
Ser59	H-bond (Acceptor)	0.20%
Arg61	H-bond (Donor)	3.59%
Arg61	Ionic (Cation)	4.39%
Trp62	Aromatic (Edge to face)	12.57%
Trp62	Aromatic (Face to face)	1.00%
Trp62	H-bond (Donor)	0.20%
Ser106	H-bond (Donor)	1.60%
Glu206	H-bond (Acceptor)	0.80%
Phe357	Aromatic (Edge to face)	0.60%
Phe357	Aromatic (Face to face)	2.00%
Ser460	H-bond (Acceptor)	0.40%
Lys463	H-bond (Donor)	6.59%
Lys463	Ionic (Cation)	5.59%
Glu464	H-bond (Acceptor)	1.60%
Arg471	H-bond (Donor)	2.20%
Arg471	Ionic (Cation)	2.79%
Ser473	H-bond (Acceptor)	0.20%
Tyr547	Aromatic (Face to face)	0.60%
Lys554	H-bond (Donor)	0.80%
Lys554	Ionic (Cation)	1.20%
Arg560	H-bond (Donor)	1.20%
Arg560	Ionic (Cation)	1.40%
Asn562	H-bond (Donor)	1.20%
Tyr666	Aromatic (Edge to face)	1.60%
Tyr666	Aromatic (Face to face)	0.40%

#### 2.4. Molecular Dynamics and Interaction Hotspot Identifications of Caffeic Acid-MMP-9

Figure 2 illustrates the interaction stability of caffeic acid in the MMP-9 active site and the conformational stability of MMP-9 backbone atoms described with the alterations of the RMSD value. Our visual inspection exhibited that at the initial simulation time, caffeic acid interacted with amino acid residues of His226, Glu227, His236, and Pro246, which were reported as the catalytic domain of MMP-9 [43]. Unlike caffeic acid in the DPP-4 active site, caffeic acid comparatively stably interacted in the MMP-9 active site even though there were RMSD fluctuations reaching more than 2.000 Å.

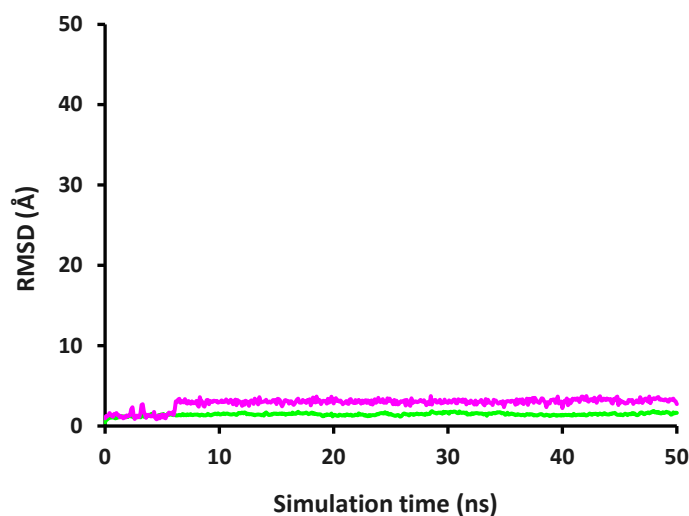


**Figure 2.** RMSD alterations of MMP-9 backbone atoms complexed with caffeic acid (green) and RMSD ligand movement of caffeic acid (purple) during 50-ns simulations.

It can be obviously observed in Figure 2 that caffeic acid interacted stably in the MMP-9 active site with an RMSD value below 2.000 Å until the simulation time reached 2.2 ns. From this simulation time, the RMSD value fluctuated until 6 ns with a maximum RMSD value of 2.708 Å. Starting from 6 ns to the end of the simulation, the RMSD value increased and continuously fluctuated, ranging from 1.373 to 3.729 Å. Even though it was found that the highest RMSD value was 3.729 Å at 42.1 ns, our findings suggested at that simulation time caffeic acid still interacted in the MMP-9 active site binding with amino acid residues of His226, Glu227, and His236. As expected, our results revealed that the carboxyl group of caffeic acid interacted with the  $Zn^{2+}$  ion throughout the simulation time via electrostatic interactions, denoting that caffeic acid has the same mechanism of MMP-9 inhibition as the other inhibitors previously reported [33]. Figure 2 also depicts the alterations of the RMSD value of MMP-9 backbone atoms having a value RMSD of  $\leq 2.000$  Å throughout the simulation, showing the stability of MMP-9 backbone atoms.

As tabulated in Table 3, PyPLIF HIPPOS 0.2.0 generated interaction hotspots of caffeic acid in the active site of MMP-9, revealing that His226 forming aromatic edge-to-face, aromatic face-to-face, and hydrophobic interactions were the interaction hotspots throughout the simulation. It was also observed that caffeic acid nicely interacted with Pro246 via hydrophobic interaction even though this amino acid had a minor contribution in stabilizing the interaction throughout the simulation. Our findings indicated that interaction with His226 had a major contribution to receptor–ligand stabilization, showing the importance of the aromatic group of caffeic acid in inhibiting MMP-9.

**Table 3.** Interaction hotspots resulted from 50-ns molecular dynamics simulations of caffeic acid in the active site of MMP-9.

Interacting Residues	Interaction Type	Interaction Percentage
His226	Aromatic (Edge-to-face)	15.56%
	Aromatic (Face-to-face)	73.85%
	Hydrophobic	90.01%
	H-bond (Donor)	1.79%
Pro246	Hydrophobic	0.79%

According to the results of the molecular dynamics simulations (Tables 1–3), the feature of caffeic acid that is responsible for the inhibitory activity of both DPP-4 and MMP-9 was the presence of the aromatic moiety. This moiety interacts with Trp62 in the allosteric site of DPP-4 and His226 in the active site of MMP-9. Moreover, the presence of

the carboxylic acid makes caffeic acid it possible to perform hydrogen bonds with either Trp62, Ser460, or Lys463 and an ionic interaction with Lys463 in the DPP-4 allosteric site. This carboxylic acid moiety could act as an electron-withdrawing group into the aromatic moiety of caffeic acid. This aromatic moiety could increase the aromatic interactions of caffeic acid to His226 of MMP-9. These features were also observed in the flavonoids that have inhibitory activity to DPP-4 and MMP-9 [44,45]. Hence, it is of considerable interest to take into account these findings in the design of dual active DPP-4 and MMP-9 inhibitors.

### 3. Materials and Methods

#### 3.1. Chemicals

Caffeic acid (CAS No.: 331-39-5) was purchased from Sigma-Aldrich (St. Louis, MO, USA). Robusta coffee (Excelso<sup>®</sup> Robusta Gold) was purchased from Kapal Api Grup, Jakarta, Indonesia. The DPP-4 inhibitor screening assay kit (Cayman Chemical, Ann Arbor, MI, USA) and MMP-9 inhibitor screening kit (Biovision K844-100) were used in this study. Dimethyl sulfoxide (DMSO), methanol, and ethyl acetate were also purchased from Sigma-Aldrich; distilled water was used as the solvent.

#### 3.2. In Silico Instrumentations

A PC client having computer specifications of AMD Ryzen 7 4800H central processing unit, NVIDIA GeForce GTX 1650 Ti graphics processing unit, 16 GB of RAM, and 512 GB of SSD was used to perform all molecular docking simulations and identify receptor–ligand interaction hotspots resulting from molecular dynamics snapshots using PyPLIF HIPPOS 0.2.0. In addition, molecular dynamics simulations were conducted using a PC having specifications of AMD Ryzen 7 5800X central processing unit, NVIDIA GeForce GTX 1650 graphics processing unit, 32 GB of RAM, and 466 GB of SSD.

#### 3.3. Standard Caffeic Acid and Sample Preparation

Preparation of standard caffeic acid and sample were developed according to the previous study [10]. Stock solutions of caffeic acid were prepared in methanol solvent. Then, 5 g of robusta coffee were accurately weighed and placed in a beaker glass followed by dilution using 200 mL of water (60 °C). This solution was then stirred four times followed by brewing for 5 min. The filtrate was separated and dried for 24 h at 60 °C. Three grams of spent coffee grounds was placed in a beaker glass and diluted with ethanol–water (40:60 *v/v*) for 2 h followed by stirring at 350 rpm and temperature of 60 °C. The obtained concentrate was then processed by applying liquid–liquid extraction using ethyl acetate (20 mL × 3). The achieved residue was diluted using methanol.

#### 3.4. DPP-4 Inhibitory Assay

The tested samples were dissolved and diluted using DMSO to the required concentration (500; 250; 125; 62.5; and 31.25 μM for caffeic acid and 500; 250; 100; 50; and 10 μg for ethanolic extract of spent coffee grounds in 100 μL assay final volume). The assay procedure is described briefly according to the manufacturer's protocols as follows: diluted assay buffer (30 μL) and diluted enzyme solution (10 μL) were added to the 96-well plate containing 10 μL of solvent (negative control), sitagliptin (positive control), or test samples. As for the background well, the diluted enzyme solution was replaced by a diluted assay buffer. The reaction was initiated by adding 50 μL of a diluted substrate solution and the plate was incubated for 30 min at 37 °C. After incubation, fluorescence was read using a Synergy HTX-3 multimode reader at 350/450 nm. The percent inhibition was determined by the formula shown in Equation (1) and the IC<sub>50</sub> can be calculated from linear regression log concentration vs percent inhibition.

$$\text{Inhibition (\%)} = \left( \frac{\text{Negative control} - \text{Inhibitor}}{\text{Negative control}} \right) \times 100\% \quad (1)$$

### 3.5. MMP-9 Inhibitory Assay

A caffeic acid with a concentration of 250; 125; 62.5; and 31.25  $\mu\text{M}$  and ethanolic extract of spent coffee grounds of 500; 250; 100; 50; and 10  $\mu\text{g}$  in 100  $\mu\text{L}$  assay final volume. The assay procedure is described briefly according to the manufacturer's protocols as follows: the enzyme control was prepared by mixing 5  $\mu\text{L}$  of the diluted MMP-9 with 45  $\mu\text{L}$  buffer. The background control was prepared with 50  $\mu\text{L}$  of buffer alone. Samples were prepared by mixing 1  $\mu\text{L}$  sample with 5  $\mu\text{L}$  diluted MMP-9 and 44  $\mu\text{L}$  buffer while solvent control was prepared with the same method as the sample by adding 1  $\mu\text{L}$  DMSO. The positive control was prepared by mixing 2  $\mu\text{L}$  NNGH with 5  $\mu\text{L}$  diluted MMP-9 and 43  $\mu\text{L}$  buffer. The reaction was initiated by adding 50  $\mu\text{L}$  of a diluted substrate solution. The fluorescence was read using a Synergy HTX-3 multimode reader at 325/393 nm in a kinetic mode at 37  $^{\circ}\text{C}$  for 60 min. Two time points were chosen in the linear range of enzyme kinetics to obtain the corresponding  $\Delta$  relative fluorescence unit or RFU (RFU2-RFU1) during the reaction time  $\Delta t$  (at least 10 min apart). These values are used to obtain the percentage of inhibition which is formulated in Equation (2).

$$\text{Relative Inhibition (\%)} = \frac{\Delta\text{RFU}(\text{ec}) - \Delta\text{RFU}(\text{sample})}{\Delta\text{RFU}(\text{ec})} \times 100\% \quad (2)$$

### 3.6. Receptor–Ligand Preparation

The crystal structure of the receptors, namely DPP-4 complexed with its native ligand, i.e., alogliptin (PDB ID: 3G0B) and MMP-9 complexed with its native ligand, i.e., CC27 (PDB ID: 4H3X), were downloaded directly to the YASARA-structure. The DPP-4 receptor was prepared by omitting unimportant residues (Nag) and solvent molecules (Hoh) while chain A was selected for further simulations. Subsequently, the pH value was adjusted to physiological pH with the commands of *pH value = 7.4, update = yes, and CleanAll* to add hydrogen atoms correctly at the determined pH. The energy minimization was performed using commands of *Options > Choose Experiment > Energy minimization*. This prepared structure, DPP-4 complexed with alogliptin, was saved as 3G0B-corr-min.yob in the working directory.

The MMP-9 receptor was prepared by omitting its solvent molecules (Hoh) and unimportant residues (Peg, Pgo, Gol,  $\text{Ca}^{2+}$ , and  $\text{Zn}^{2+}$  which are not complexed with the native ligand) while chain A was selected for further simulations. In this preparation, we discovered that YASARA cannot identify the single bond of the NH-OH group of the native ligand. Therefore, we manually corrected it by adjusting the system pH to physiological pH with a command of *pH value = 7.4, update = yes, and CleanAll* and editing that bond from double bond to single bond with a command of *DelBond 2669,2668* followed by a command of *AddBond 2669, 2668* and *AddHyd* all using the YASARA-console. Finally, energy minimization was also performed using the same commands as DPP-4 preparation and the  $\text{Zn}^{2+}$  object was joined to the receptor, becoming one object containing the receptor and the  $\text{Zn}^{2+}$ . The prepared structure of MMP-9 complexed with CC27 was saved as 4H3X-corr-min.yob in a different working directory.

### 3.7. Redocking of the Native Ligand

Redocking of the native ligand was carried out to validate the proposed molecular docking configuration [46]. Redocking of each native ligand for each receptor was conducted using our in-house developed YASARA plug-in which enabled us to perform 100 redocking simulations. The prepared and corrected receptor–ligand complex file, 3G0B-corr-min.yob and 4H3X-corr-min.yob, was individually set as the MacroTarget for our in-house developed YASARA plug-in. The processes involved in our in-house developed YASARA plug-in are: (1) the receptor–ligand complex was separated into two objects which were object 1 as the receptor and object 2 as the native ligand, respectively. At the same time, this process also constructed object 3, which was a cubic simulation cell with a distance of 5.000  $\text{\AA}$  from the native ligand outer atoms. (2) Afterward, object 2 was



saved individually as a YASARA object file with the file name of MacroTarget\_ref.yob and MacroTarget\_ligand.yob then object 2 was deleted from the YASARA-structure. (3) Another file was generated, i.e., MacroTarget\_receptor.sce, containing the receptor structure and the simulation cell. Subsequently, 100 redocking simulations of MacroTarget\_ligand.yob and MacroTarget\_receptor.sce were performed using the AutoDock Vina scoring function [47]. Eventually, the root-mean-square deviation (RMSD) of the best-docked native ligand from each simulation was calculated, comparing the heavy atom coordinate and native ligand conformation to the co-crystallized native ligand structure as saved as MacroTarget\_ref.yob. Our in-house developed YASARA plug-in also generated a file named MacroTarget\_config.mcr containing the redocking configuration, which could be used for the molecular docking configuration of the proposed compound, i.e., caffeic acid, with the same configuration as the redocking.

### 3.8. Molecular Docking of Caffeic Acid

Molecular docking of caffeic acid targeting the DPP-4 and MMP-9 active sites was conducted separately in a different working directory. MacroTarget\_receptor.sce and MacroTarget\_config.mcr resulted from the redocking of each native ligand and were copied as the files generated from each redocking process. The three-dimensional structure of caffeic acid was built using the YASARA-structure and its SMILES code of C1=CC(=C(C=C1C=CC(=O)O)O)O. The pH system was also adjusted to physiological pH with a command of *pH value = 7.4, update = yes, and CleanAll* and then to add hydrogen atoms in that desired pH condition. The energy minimization was performed using commands of *Options > Choose Experiment > Energy minimization*. This 3D molecular model of caffeic acid was then saved as 3G0B-corr-min.yob and 4H3X-corr-min.yob as the prepared molecular model to perform molecular docking in the DPP-4 and MMP-9 active sites, respectively. Each file was set as the MacroTarget for our other in-house developed YASARA plug-in on YASARA-structure, allowing us to set the molecular docking configuration as the redocking configuration which was set in MacroTarget\_config.mcr file. Thereafter, our subsequent in-house developed YASARA plug-in was run to perform 100 molecular docking simulations. At last, the RMSD value of the best-docked caffeic acid was calculated, comparing the heavy atom coordinate and conformation of the best-docked caffeic acid from each simulation with the best-docked caffeic acid from the first simulation. This RMSD calculation was run using our next in-house developed YASARA plug-in resulting in a file named rmsd\_bestpose\_all.txt. The best-docked caffeic acid which possessed an RMSD value  $> 2.000 \text{ \AA}$  denoted that the best-docked caffeic acid conformation could be distinguishable from the best-docked caffeic acid resulted from the first simulation.

### 3.9. Molecular Dynamics Simulations

The interaction stability of the best-docked caffeic acid in the active site of DPP-4 and MMP-9 was evaluated using molecular dynamics simulations which were executed using the YASARA-structure. Molecular dynamics simulations were performed using the AMBER14 force field. The solvation system was set in the  $10 \times 10 \times 10 \text{ \AA}^3$  cubic cell and a periodic boundary condition (PBC) was maintained during the simulations with water density of  $0.993 \text{ g/mL}$  at  $310 \text{ K}$  in the pressure of  $1 \text{ bar}$ . The system was neutralized by the addition of counter ions,  $\text{Na}^+$  and  $\text{Cl}^-$ , with a concentration of  $0.9\%$  and the pH was set to  $7.4$  as the physiological condition. The system was then subjected to energy minimization using the steepest descent and simulated annealing to remove steric clashes. The particle mesh Ewald (PME) algorithm with no cut-off was used to describe the long-range electrostatic interactions whereas the van der Waals interactions cut-off was  $8.00 \text{ \AA}$ . Finally, molecular dynamics simulations of each system were carried out in  $50\text{-ns}$  with a time step of  $2.5\text{-fs}$  and the snapshot was saved every  $100\text{-ps}$ . The molecular dynamics simulations resulted in root-mean-square deviation of receptor backbone atoms (RMSD-backbone) and root-mean-square deviation of ligand movement (RMSD-LigMove) which were then further analyzed to evaluate the stability of receptor–ligand interactions.

### 3.10. Interaction Hotspot Identifications

The identification of interaction fingerprints was carried out using PyPLIF HIPPOS 0.2.0., which is the new version of PyPLIF HIPPOS [24]. The snapshots resulting from the molecular dynamics simulations (see Section 3.9) were converted into pdb format. Subsequently, the molecular dynamics snapshots in pdb format were analyzed automatically using the new feature direct IFP from PyPLIF HIPPOS 0.2.0 to identify interaction fingerprints of caffeic acid interacting with DPP-4 and MMP-9 throughout the simulations. The resulting interaction fingerprints were grouped based on the interaction type to calculate the interaction hotspots.

## 4. Conclusions

Caffeic acid and the ethanolic extract of spent coffee grounds could potentially act as dual inhibitors targeting DPP-4 and MMP-9 as alternative treatments for type 2 diabetes mellitus and diabetic foot ulcers. Molecular dynamics simulations denoted that caffeic acid interacted in the plausible allosteric site of DPP-4 and the active site of MMP-9, which could support the in vitro experimental data. PyPLIF HIPPOS 0.2.0 successfully identified the interaction hotspots of caffeic acid interacting with DPP-4 and MMP-9 throughout 50-ns molecular dynamics simulations, which exhibited the predominant interactions reinforcing the receptor–ligand interactions. Our findings also provide the new version of PyPLIF HIPPOS, i.e., PyPLIF HIPPOS 0.2.0 which can be further used to support structure-based drug discovery.

**Author Contributions:** Funding acquisition, E.P.I., N.Y., V.D.P. and S.M.; conceptualization, E.P.I., F.D.O.R. and V.D.P.; methodology, E.P.I. and M.R.S.Y.; software, E.P.I.; validation, S.S.W.W. and E.P.I.; formal analysis, E.P.I.; investigation, E.P.I.; writing—original draft preparation, S.S.W.W. and F.D.O.R.; writing—review and editing, N.Y., V.D.P. and S.M.; project administration, E.P.I. and M.R.S.Y. All authors have read and agreed to the published version of the manuscript.

**Funding:** This research was funded by the Directorate of Research, Technology, and Community Services, the Directorate General of Higher Education, Research, and Technology, the Indonesian Ministry of Education, Culture, Research, and Technology (No. 075/E5/PG.02.00.PL/2023).

**Institutional Review Board Statement:** Not applicable.

**Informed Consent Statement:** Not applicable.

**Data Availability Statement:** The data presented in this study are available on request from the corresponding author.

**Acknowledgments:** Muhammad Radifar is acknowledged for technically maintaining PyPLIF HIPPOS (<https://github.com/radifar/PyPLIF-HIPPOS>, accessed on 16 August 2023).

**Conflicts of Interest:** The authors declare no conflict of interest.

**Sample Availability:** Samples of the compounds are available from the authors.

## References

1. Westman, E.C. Type 2 Diabetes Mellitus: A Pathophysiologic Perspective. *Front. Nutr.* **2021**, *8*, 707371. [[CrossRef](#)] [[PubMed](#)]
2. Donath, M.Y.; Ehses, J.A.; Maedler, K.; Schumann, D.M.; Ellingsgaard, H.; Eppler, E.; Reinecke, M. Mechanisms of  $\beta$ -Cell Death in Type 2 Diabetes. *Diabetes* **2005**, *54*, S108–S113. [[CrossRef](#)] [[PubMed](#)]
3. Mariadoss, A.V.A.; Sivakumar, A.S.; Lee, C.H.; Kim, S.J. Diabetes Mellitus and Diabetic Foot Ulcer: Etiology, Biochemical and Molecular Based Treatment Strategies via Gene and Nanotherapy. *Biomed. Pharmacother.* **2022**, *151*, 113134. [[CrossRef](#)]
4. Diabetes Facets and Figures. International Diabetes Federation. Available online: <https://idf.org/about-diabetes/diabetes-facts-figures/> (accessed on 3 September 2023).
5. Pang, B.; Zhou, Q.; Li, J.L.; Zhao, L.H.; Tong, X.L. Treatment of Refractory Diabetic Gastroparesis: Western Medicine and Traditional Chinese Medicine Therapies. *World J. Gastroenterol.* **2014**, *20*, 6504–6514. [[CrossRef](#)] [[PubMed](#)]
6. Xu, L.; Li, Y.; Dai, Y.; Peng, J. Natural Products for the Treatment of Type 2 Diabetes Mellitus: Pharmacology and Mechanisms. *Pharmacol. Res.* **2018**, *130*, 451–465. [[CrossRef](#)]
7. Herman, A.; Herman, A.P. Herbal Products and Their Active Constituents for Diabetic Wound Healing—Preclinical and Clinical Studies: A Systematic Review. *Pharmaceutics* **2023**, *15*, 281. [[CrossRef](#)] [[PubMed](#)]

8. Yuan, H.; Ma, Q.; Ye, L.; Piao, G. The Traditional Medicine and Modern Medicine from Natural Products. *Molecules* **2016**, *21*, 559. [[CrossRef](#)] [[PubMed](#)]
9. Monteiro Espíndola, K.M.; Ferreira, R.G.; Mosquera Narvaez, L.E.; Rocha Silva Rosario, A.C.; Machado Da Silva, A.H.; Bispo Silva, A.G.; Oliveira Vieira, A.P.; Chagas Monteiro, M. Chemical and Pharmacological Aspects of Caffeic Acid and Its Activity in Hepatocarcinoma. *Front. Oncol.* **2019**, *9*, 467241. [[CrossRef](#)]
10. Gani, M.R.; Istyastono, E.P. Determination of Caffeic Acid in Ethanolic Extract of Spent Coffee Grounds by High-Performance Liquid Chromatography with UV Detection. *Indones. J. Chem.* **2021**, *21*, 1281–1286. [[CrossRef](#)]
11. Spagnol, C.M.; Assis, R.P.; Brunetti, I.L.; Isaac, V.L.B.; Salgado, H.R.N.; Corrêa, M.A. In Vitro Methods to Determine the Antioxidant Activity of Caffeic Acid. *Spectrochim. Acta Part A Mol. Biomol. Spectrosc.* **2019**, *219*, 358–366. [[CrossRef](#)]
12. Saivish, M.V.; Pacca, C.C.; da Costa, V.G.; de Lima Menezes, G.; da Silva, R.A.; Nebo, L.; da Silva, G.C.D.; de Aguiar Milhim, B.H.G.; da Silva Teixeira, I.; Henrique, T.; et al. Caffeic Acid Has Antiviral Activity against Ilhéus Virus In Vitro. *Viruses* **2023**, *15*, 494. [[CrossRef](#)] [[PubMed](#)]
13. Bai, X.; Li, S.; Liu, X.; An, H.; Kang, X.; Guo, S. Caffeic Acid, an Active Ingredient in Coffee, Combines with DOX for Multitarget Combination Therapy of Lung Cancer. *J. Agric. Food Chem.* **2022**, *70*, 8326–8337. [[CrossRef](#)] [[PubMed](#)]
14. Alson, S.G.; Jansen, O.; Cieckiewicz, E.; Rakotoarimanana, H.; Rafatro, H.; Degotte, G.; Francotte, P.; Frederich, M. In-Vitro and in-Vivo Antimalarial Activity of Caffeic Acid and Some of Its Derivatives. *J. Pharm. Pharmacol.* **2018**, *70*, 1349–1356. [[CrossRef](#)] [[PubMed](#)]
15. Oršolić, N.; Sirovina, D.; Odeh, D.; Gajski, G.; Balta, V.; Šver, L.; Jembrek, M.J. Efficacy of Caffeic Acid on Diabetes and Its Complications in the Mouse. *Molecules* **2021**, *26*, 3262. [[CrossRef](#)] [[PubMed](#)]
16. Salau, V.F.; Erukainure, O.L.; Ijomone, O.M.; Islam, M.S. Caffeic Acid Regulates Glucose Homeostasis and Inhibits Purinergic and Cholinergic Activities While Abating Oxidative Stress and Dyslipidaemia in Fructose-Streptozotocin-Induced Diabetic Rats. *J. Pharm. Pharmacol.* **2022**, *74*, 973–984. [[CrossRef](#)] [[PubMed](#)]
17. Huang, D.W.; Shen, S.C. Caffeic Acid and Cinnamic Acid Ameliorate Glucose Metabolism via Modulating Glycogenesis and Gluconeogenesis in Insulin-Resistant Mouse Hepatocytes. *J. Funct. Foods* **2012**, *4*, 358–366. [[CrossRef](#)]
18. Shaikh, S.; Lee, E.J.; Ahmad, K.; Ahmad, S.S.; Lim, J.H.; Choi, I. A Comprehensive Review and Perspective on Natural Sources as Dipeptidyl Peptidase-4 Inhibitors for Management of Diabetes. *Pharmaceuticals* **2021**, *14*, 591. [[CrossRef](#)]
19. Hariono, M.; Yuliani, S.H.; Istyastono, E.P.; Riswanto, F.D.O.; Adhipandito, C.F. Matrix Metalloproteinase 9 (MMP9) in Wound Healing of Diabetic Foot Ulcer: Molecular Target and Structure-Based Drug Design. *Wound Med.* **2018**, *22*, 1–13. [[CrossRef](#)]
20. Wang, L.; Li, X.; Zhang, S.; Lu, W.; Liao, S.; Liu, X.; Shan, L.; Shen, X.; Jiang, H.; Zhang, W.; et al. Natural Products as a Gold Mine for Selective Matrix Metalloproteinases Inhibitors. *Bioorg. Med. Chem.* **2012**, *20*, 4164–4171. [[CrossRef](#)]
21. Chen, J.; Qin, S.; Liu, S.; Zhong, K.; Jing, Y.; Wu, X.; Peng, F.; Li, D.; Peng, C. Targeting Matrix Metalloproteases in Diabetic Wound Healing. *Front. Immunol.* **2023**, *14*, 1089001. [[CrossRef](#)]
22. Fan, S.L.; Lin, J.A.; Chen, S.Y.; Lin, J.H.; Lin, H.T.; Chen, Y.Y.; Yen, G.C. Effects of Hsian-Tsao (*Mesona procumbens* Hemsl.) Extracts and Its Polysaccharides on the Promotion of Wound Healing under Diabetes-like Conditions. *Food Funct.* **2021**, *12*, 119–132. [[CrossRef](#)]
23. Istyastono, E.P.; Riswanto, F.D.O. Molecular Dynamics Simulations of the Caffeic Acid Interactions to Dipeptidyl Peptidase Iv. *Int. J. Appl. Pharm.* **2022**, *14*, 274–278. [[CrossRef](#)]
24. Istyastono, E.P.; Radifar, M.; Yuniarti, N.; Prasasty, V.D.; Mungkasi, S. PyPLIF HIPPOS: A Molecular Interaction Fingerprinting Tool for Docking Results of AutoDock Vina and PLANTS. *J. Chem. Inf. Model.* **2020**, *60*, 3697–3702. [[CrossRef](#)]
25. Saberian, M.; Li, J.; Donnoli, A.; Bonderenko, E.; Oliva, P.; Gill, B.; Lockrey, S.; Siddique, R. Recycling of Spent Coffee Grounds in Construction Materials: A Review. *J. Clean. Prod.* **2021**, *289*, 125837. [[CrossRef](#)]
26. Campos-Vega, R.; Loarca-Piña, G.; Vergara-Castañeda, H.A.; Dave Oomah, B. Spent Coffee Grounds: A Review on Current Research and Future Prospects. *Trends Food Sci. Technol.* **2015**, *45*, 24–36. [[CrossRef](#)]
27. Franca, A.S.; Oliveira, L.S. Potential Uses of Spent Coffee Grounds in the Food Industry. *Foods* **2022**, *11*, 2064. [[CrossRef](#)] [[PubMed](#)]
28. Biftu, T.; Sinha-Roy, R.; Chen, P.; Qian, X.; Feng, D.; Kuethe, J.T.; Scapin, G.; Gao, Y.D.; Yan, Y.; Krueger, D.; et al. Omarigliptin (MK-3102): A Novel Long-Acting DPP-4 Inhibitor for Once-Weekly Treatment of Type 2 Diabetes. *J. Med. Chem.* **2014**, *57*, 3205–3212. [[CrossRef](#)]
29. Mourad, A.A.E.; Khodir, A.E.; Saber, S.; Mourad, M.A.E. Novel Potent and Selective DPP-4 Inhibitors: Design, Synthesis and Molecular Docking Study of Dihydropyrimidine Phthalimide Hybrids. *Pharmaceuticals* **2021**, *14*, 144. [[CrossRef](#)]
30. Lin, Y.S.; Chen, C.R.; Wu, W.H.; Wen, C.L.; Chang, C.I.; Hou, W.C. Anti- $\alpha$ -Glucosidase and Anti-Dipeptidyl Peptidase-IV Activities of Extracts and Purified Compounds from *Vitis Thunbergii* Var. *Taiwaniana*. *J. Agric. Food Chem.* **2015**, *63*, 6393–6401. [[CrossRef](#)]
31. Gupta, A.; Jacobson, G.A.; Burgess, J.R.; Jelinek, H.F.; Nichols, D.S.; Narkowicz, C.K.; Al-Aubaidy, H.A. Citrus Bioflavonoids Dipeptidyl Peptidase-4 Inhibition Compared with Gliptin Antidiabetic Medications. *Biochem. Biophys. Res. Commun.* **2018**, *503*, 21–25. [[CrossRef](#)]
32. Majeed, M.; Majeed, S.; Mundkur, L.; Nagabhusanam, K.; Arumugam, S.; Beede, K.; Ali, F. Standardized *Emblca Officinalis* Fruit Extract Inhibited the Activities of  $\alpha$ -Amylase,  $\alpha$ -Glucosidase, and Dipeptidyl Peptidase-4 and Displayed Antioxidant Potential. *J. Sci. Food Agric.* **2020**, *100*, 509–516. [[CrossRef](#)] [[PubMed](#)]

33. Laronha, H.; Carpinteiro, I.; Portugal, J.; Azul, A.; Polido, M.; Petrova, K.T.; Salema-Oom, M.; Caldeira, J. Challenges in Matrix Metalloproteinases Inhibition. *Biomolecules* **2020**, *10*, 717. [[CrossRef](#)] [[PubMed](#)]
34. Crasci, L.; Basile, L.; Panico, A.; Puglia, C.; Bonina, F.P.; Basile, P.M.; Rizza, L.; Guccione, S. Correlating in Vitro Target-Oriented Screening and Docking: Inhibition of Matrix Metalloproteinases Activities by Flavonoids. *Planta Med.* **2017**, *83*, 901–911. [[CrossRef](#)] [[PubMed](#)]
35. Saragusti, A.C.; Ortega, M.G.; Cabrera, J.L.; Estrin, D.A.; Marti, M.A.; Chiabrando, G.A. Inhibitory Effect of Quercetin on Matrix Metalloproteinase 9 Activity Molecular Mechanism and Structure-Activity Relationship of the Flavonoid-Enzyme Interaction. *Eur. J. Pharmacol.* **2010**, *644*, 138–145. [[CrossRef](#)] [[PubMed](#)]
36. Hariono, M.; Rollando, R.; Karamoy, J.; Hariyono, P.; Salin, N.; Wahab, H. Bioguided Fractionation of Local Plants against Matrix Metalloproteinase9 and Its Cytotoxicity against Breast Cell Models: In Silico and In Vitro Study. *Molecules* **2020**, *25*, 4691. [[CrossRef](#)]
37. Chen, Y.C. Beware of Docking! *Trends Pharmacol. Sci.* **2015**, *36*, 78–95. [[CrossRef](#)]
38. Liu, K.; Kokubo, H. Exploring the Stability of Ligand Binding Modes to Proteins by Molecular Dynamics Simulations: A Cross-Docking Study. *J. Chem. Inf. Model.* **2017**, *57*, 2514–2522. [[CrossRef](#)]
39. Musoev, A.; Numonov, S.; You, Z.; Gao, H. Discovery of Novel DPP-IV Inhibitors as Potential Candidates for the Treatment of Type 2 Diabetes Mellitus Predicted by 3D QSAR Pharmacophore Models, Molecular Docking and de Novo Evolution. *Molecules* **2019**, *24*, 2870. [[CrossRef](#)]
40. Tomovic, K.; Ilic, B.S.; Miljkovic, M.; Dimov, S.; Yancheva, D.; Kojic, M.; Mavrova, A.T.; Kocic, G.; Smelcerovic, A. Benzo[4,5]Thieno[2,3-d]Pyrimidine Phthalimide Derivative, One of the Rare Noncompetitive Inhibitors of Dipeptidyl Peptidase-4. *Arch. Pharm. Chem. Life Sci.* **2020**, *353*, 1900238. [[CrossRef](#)]
41. Nongonierma, A.B.; Mooney, C.; Shields, D.C.; Fitzgerald, R.J. In Silico Approaches to Predict the Potential of Milk Protein-Derived Peptides as Dipeptidyl Peptidase IV (DPP-IV) Inhibitors. *Peptides* **2014**, *57*, 43–51. [[CrossRef](#)]
42. Nongonierma, A.B.; Fitzgerald, R.J. Inhibition of Dipeptidyl Peptidase IV (DPP-IV) by Tryptophan Containing Dipeptides. *Food Funct.* **2013**, *4*, 1843–1849. [[CrossRef](#)] [[PubMed](#)]
43. Malekipour, M.H.; Shirani, F.; Moradi, S.; Taherkhani, A. Cinnamic Acid Derivatives as Potential Matrix Metalloproteinase-9 Inhibitors: Molecular Docking and Dynamics Simulations. *Genom. Inform.* **2023**, *21*, e9. [[CrossRef](#)] [[PubMed](#)]
44. Pan, J.; Zhang, Q.; Zhang, C.; Yang, W.; Liu, H.; Lv, Z.; Liu, J.; Jiao, Z. Inhibition of Dipeptidyl Peptidase-4 by Flavonoids: Structure–Activity Relationship, Kinetics and Interaction Mechanism. *Front. Nutr.* **2022**, *9*, 892426. [[CrossRef](#)] [[PubMed](#)]
45. Ende, C.; Gebhardt, R. Inhibition of Matrix Metalloproteinase-2 and -9 Activities by Selected Flavonoids. *Planta Med.* **2004**, *70*, 1006–1008. [[CrossRef](#)]
46. Diallo, B.N.; Swart, T.; Hoppe, H.C.; Tastan Bishop, Ö.; Lobb, K. Potential Repurposing of Four FDA Approved Compounds with Antiplasmodial Activity Identified through Proteome Scale Computational Drug Discovery and in Vitro Assay. *Sci. Rep.* **2021**, *11*, 1413. [[CrossRef](#)]
47. Trott, O.; Olson, A.J. AutoDock Vina: Improving the Speed and Accuracy of Docking with a New Scoring Function, Efficient Optimization, and Multithreading. *J. Comput. Chem.* **2010**, *31*, 455–461. [[CrossRef](#)]

**Disclaimer/Publisher’s Note:** The statements, opinions and data contained in all publications are solely those of the individual author(s) and contributor(s) and not of MDPI and/or the editor(s). MDPI and/or the editor(s) disclaim responsibility for any injury to people or property resulting from any ideas, methods, instructions or products referred to in the content.